

## Electronic Supporting Information

### Superparamagnetic-blocked state transition under alternating magnetic fields: towards determining the magnetic anisotropy in magnetic suspensions

David Cabrera<sup>1,2</sup>, Takashi Yoshida<sup>3</sup>, Teresa Rincón-Domínguez<sup>1</sup>, J.L. F. Cuñado<sup>1,4</sup>, Gorka Salas<sup>1,5</sup>, Alberto Bollero<sup>1</sup>, María del Puerto Morales<sup>6</sup>, Julio Camarero<sup>1,4</sup> and Francisco J. Teran<sup>\*1,5</sup>

<sup>1</sup> iMdea Nanociencia, Campus Universitaria de Cantoblanco, 28049 Madrid, Spain.

<sup>2</sup> School of Pharmacy and Bioengineering, Guy Hilton Research Centre, Thurnburrow Drive, ST4 7QB, Stoke on Trent, UK.

<sup>3</sup> Dpt. of Electrical Engineering, Kyushu University, Fukuoka 819-0385, Japan.

<sup>4</sup> Departamento de Física de la Materia Condensada and Instituto 'Nicolás Cabrera', Universidad Autónoma de Madrid, 28049 Madrid, Spain.

<sup>5</sup> Nanobiotecnología (iMdea Nanociencia), Unidad Asociada al Centro Nacional de Biotecnología (CSIC), 28049 Madrid, Spain

<sup>6</sup> Instituto de Ciencia de Materiales de Madrid, CSIC, Cantoblanco, 28049 Madrid, Spain

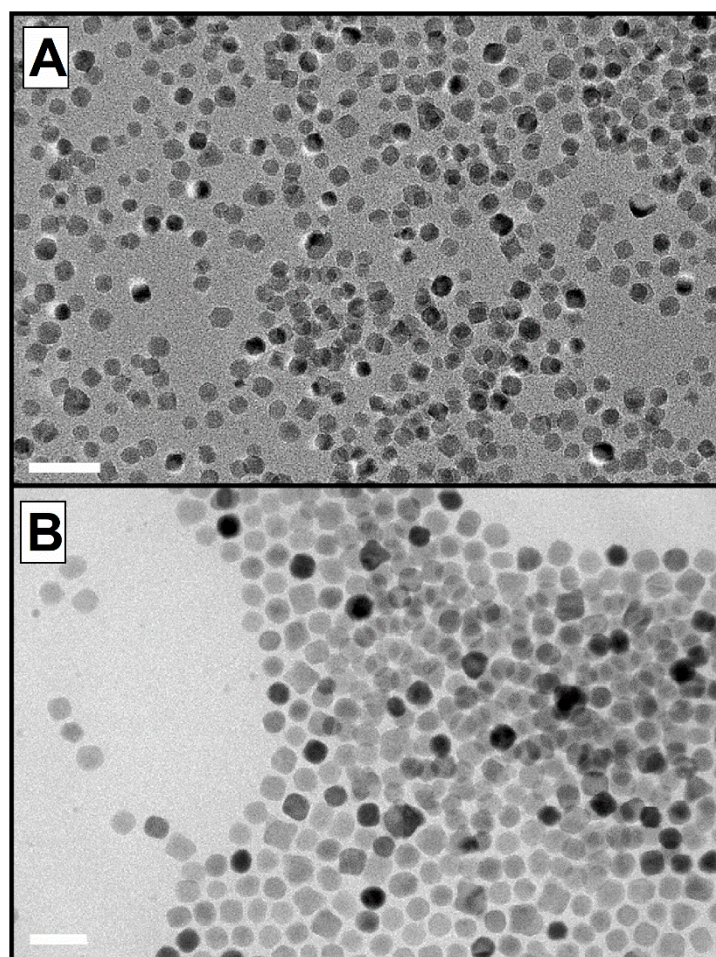


**Figure S1.** Representative TEM micrographs of (A) 12 and (B) 22 nm IONPs. Scale bar: 50 nm.

# Electronic Supporting Information

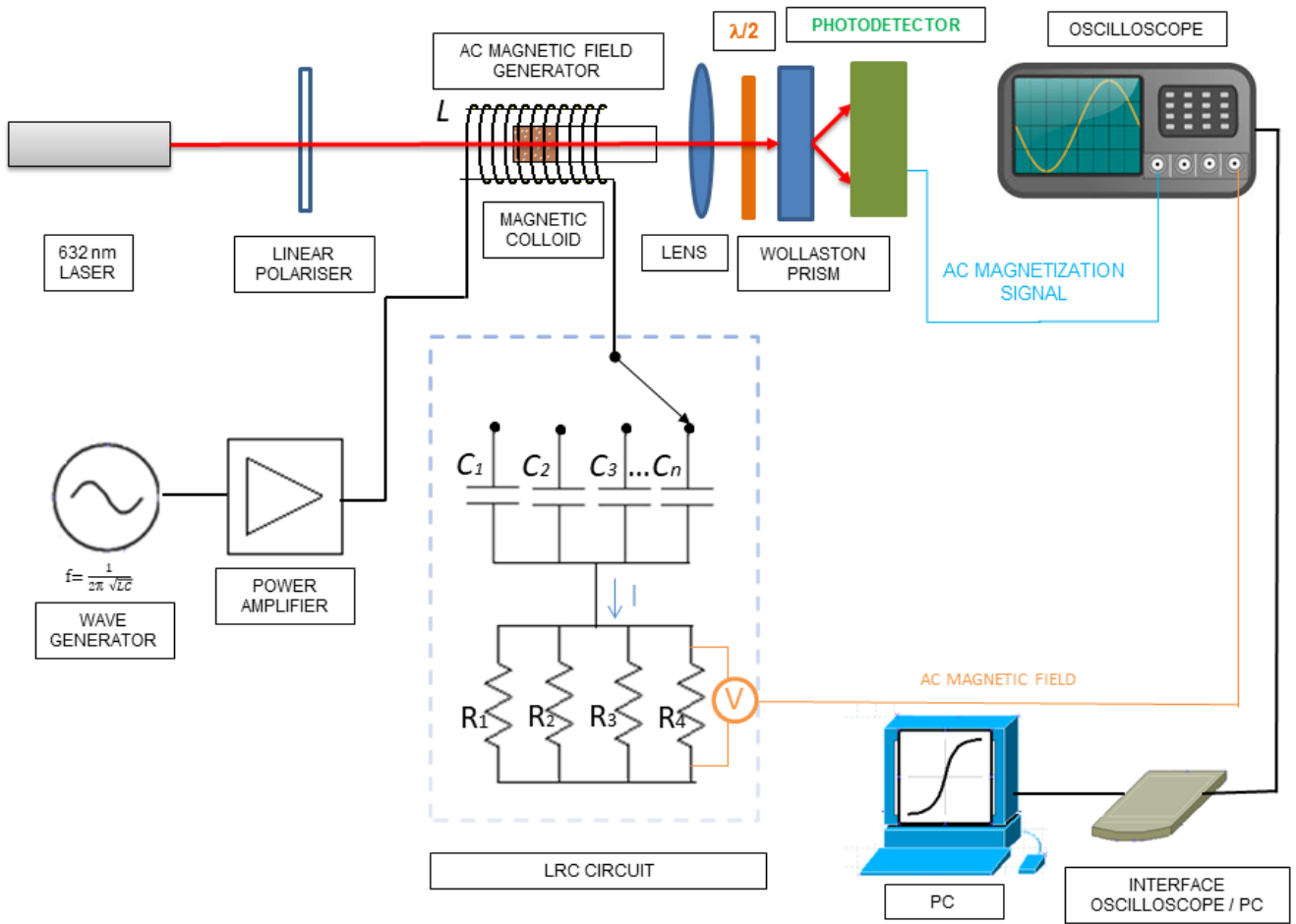


**Figure S2.** Schematic representation of magneto-optical Faraday effect magnetometer.

## Electronic Supporting Information

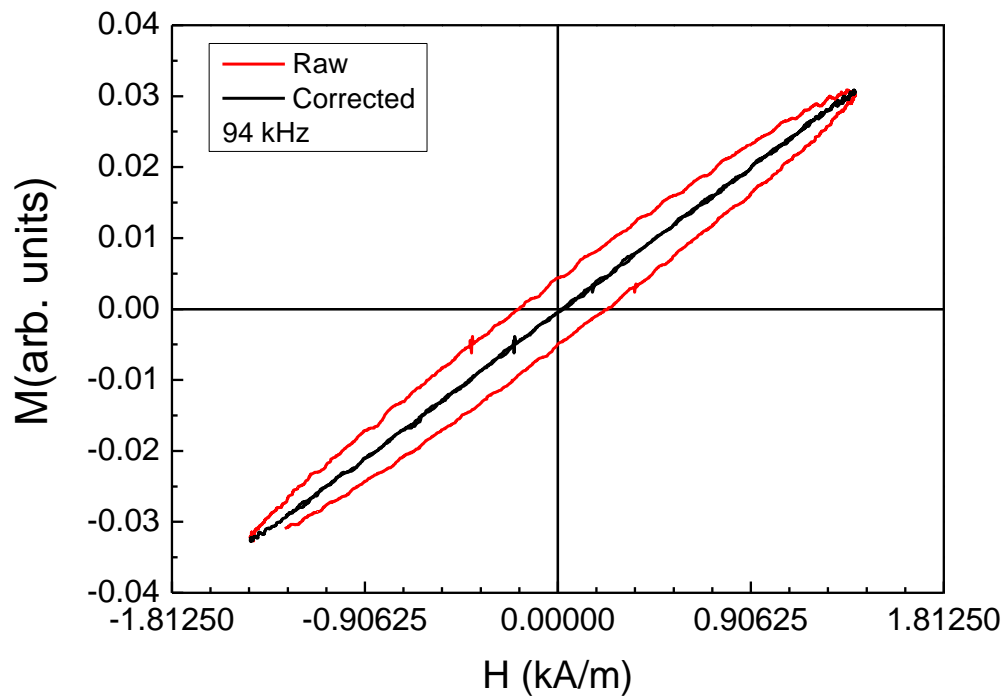


**Figure S3.** Representative MvH loops obtained in quartz crystal at 94 kHz and room temperature before and after corrections of artifacts in the input signal.

# Electronic Supporting Information

## Modified version of the Landau-Liftshitz-Gilbert (LLG) equations

The random torque  $\vec{\Gamma}$  in Eq. (2) caused by thermal fluctuations satisfies the following equations:

$$\langle \Gamma_i(t) \rangle = 0, \quad (S1)$$

$$\langle \Gamma_i(t) \Gamma_j(t') \rangle = 2\delta_{ij}\delta(t - t'). \quad (S2)$$

Here,  $\langle \rangle$  represents the average over an ensemble,  $i$  and  $j$  are Cartesian indices,  $\delta_{ij}$  is the Kronecker delta function, and  $\delta$  is the Dirac delta function.

Assuming a uniaxial magnetic anisotropy and neglecting magnetic dipolar interactions, the effective magnetic field

$\vec{H}_{\text{eff}}$  in Eq. (3) is given by

$$\vec{H}_{\text{eff}} = \vec{H}_{\text{ex}} + \vec{H}_{\text{K}}, \quad (S3)$$

$$\vec{H}_{\text{K}} = \frac{2KV_c}{\mu_0 m_{\text{NP}}} (\vec{u} \cdot \vec{n}) \vec{n}, \quad (S4)$$

where  $\vec{H}_{\text{ex}}$  and  $\vec{H}_{\text{K}}$  are the external and magnetic-anisotropy fields, respectively.

The fluctuating magnetic field,  $\vec{H}_{\text{th}}$ , due to thermal noise in Eq. (3) satisfies the following equations:

$$\langle H_{\text{th},i}(t) \rangle = 0, \quad (S5)$$

$$\langle H_{\text{th},i}(t) H_{\text{th},j}(t') \rangle = \frac{2\lambda}{1+\lambda^2} \frac{k_B T}{\mu_0^2 \gamma m_{\text{NP}}} \delta_{ij} \delta(t - t'). \quad (S6)$$

Nanoparticle core volume utilised in simulations was estimated by TEM. Nanoparticle size ( $d$ ) was determined through manual analysis of ensembles of over 300 particles found in randomly selected areas of the enlarged micrographs, with ImageTool software to obtain the mean size and standard deviation. For simulation purposes, nanoparticle volume ( $V$ ) was calculated by simplifying nanoparticle shape as spherical:

$$V = \frac{\pi d^3}{6} \quad (S7)$$

## Electronic Supporting Information

In equations 2 and 3, damping coefficient  $\lambda$  was set to 0.1 and gyromagnetic ratio  $\gamma$  was calculated using the following relationship between  $\tau_{N0}$  and  $\gamma$  :

$$\tau_{N0} = \frac{1}{2\gamma\lambda} \frac{M_s}{K} = 10^{-9} \text{ s} \quad (\text{S8})$$

Here,  $M_s$  was determined fixed from the VSM magnetisation loops and only  $K$  was considered the adjustable parameter to fit the simulations to the experimental results. Otherwise, effective magnetic field is defined in Eqs. (S3) and (S4). Size distribution was not included into Brownian and effective relaxation times.

# Electronic Supporting Information

## Comparison of simulated and experimental MvH loops

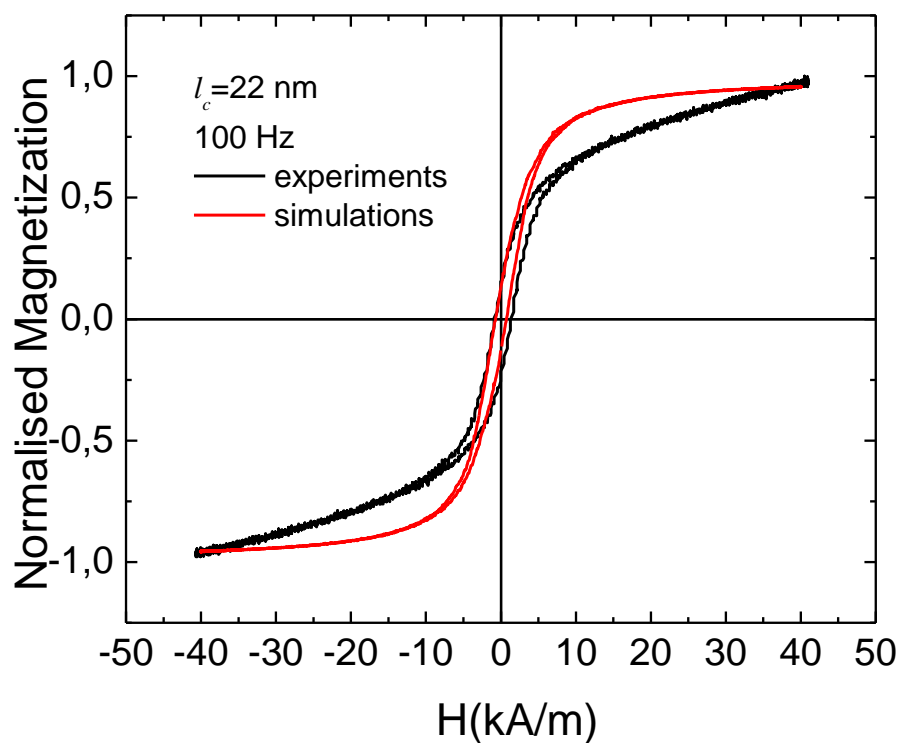


**Figure S4.** Comparison between experimental (black line) and LLG simulated (red line) AC hysteresis loops for 22 nm size IONPs dispersed in water at 0,4gFe/L, 100 Hz, and room temperature (298 K).

## Electronic Supporting Information

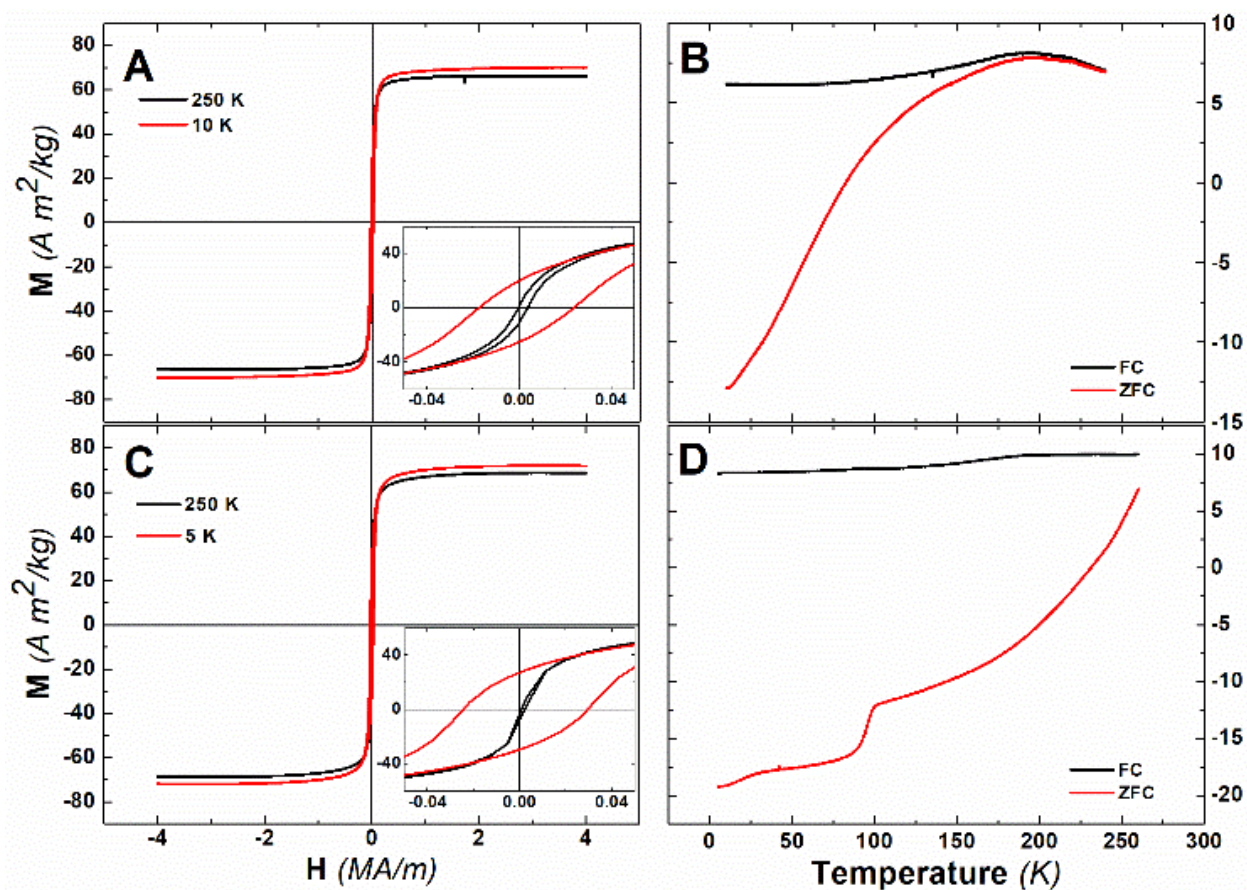


**Figure S5.-** Mass normalized magnetization cycles at different temperatures for (A) 12nm and (C) 22nm IONPs. Inset: Magnetization zoom at low magnetic fields. Zero field cooling- Field cooling measurements for (B) 12 and (D) 22 nm IONPs.

## Electronic Supporting Information

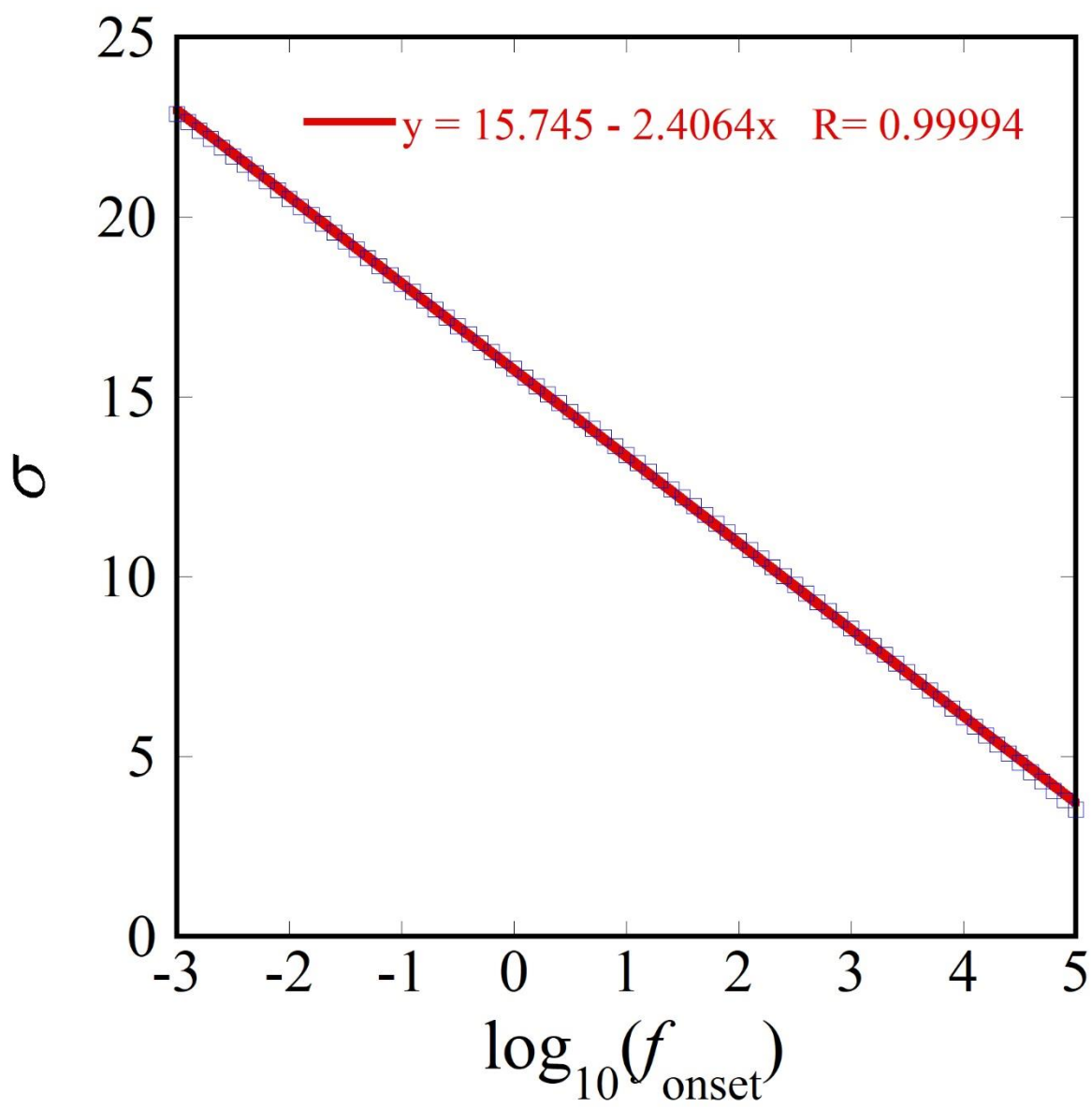


**Figure S6.** Correlation between  $f_{\text{onset}}$  and  $\sigma = K_{\text{eff}}V/k_{\text{B}}T$ .